available at www.sciencedirect.com
journal homepage: www.eu-openscience.europeanurology.com

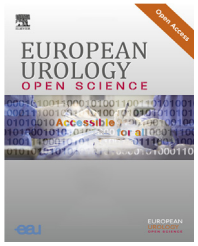

European Association of Urology

Prostate Cancer

Thresholds of Body Composition Changes Associated with Survival During Androgen Deprivation Therapy in Prostate Cancer

Pin-Chi Chen [a,†], *Pai-Kai Chiang* [b,c,d,†], *Jhen-Bin Lin* [e], *Wei-Kung Tsai* [b,c,d], *Wan-Chun Lin* [f], *Ya-Ting Jan* [b,g], *Kun-Pin Wu* [f], *Jie Lee* [b,h,*]

[a] *School of Medicine, College of Medicine, National Yang Ming Chiao Tung University, Taipei, Taiwan;* [b] *Department of Medicine, MacKay Medical College, New Taipei City, Taiwan;* [c] *Department of Urology, MacKay Memorial Hospital, Taipei, Taiwan;* [d] *MacKay Junior College of Medicine, Nursing, and Management, Taipei, Taiwan;* [e] *Department of Radiation Oncology, Changhua Christian Hospital, Changhua, Taiwan;* [f] *Institute of Biomedical Informatics, National Yang Ming Chiao Tung University, Taipei, Taiwan;* [g] *Department of Radiology, MacKay Memorial Hospital, Taipei, Taiwan;* [h] *Department of Radiation Oncology, MacKay Memorial Hospital, Taipei, Taiwan*

Article info

Article history:
Accepted October 7, 2024

Associate Editor:
Silvia Proietti

Keywords:
Prostate cancer
Androgen deprivation therapy
Body composition change
Threshold
Explainable artificial intelligence

Abstract

Background and objective: Androgen deprivation therapy (ADT) is associated with reduced muscle and increased fat mass in patients with prostate cancer. However, the threshold for body composition changes associated with survival during ADT remains unclear. This study aimed to identify body composition change thresholds for all-cause mortality during ADT.

Methods: We enrolled 538 patients with prostate cancer (332 and 206 in the derivation and external validation cohorts, respectively) who underwent radiotherapy and ADT at two tertiary centers. Computed tomography (CT) images at baseline and 6 mo after ADT initiation were retrieved for an analysis. Skeletal muscle index (SMI), subcutaneous adipose tissue index (SATI), and visceral adipose tissue index (VATI) were measured using CT at the L3 vertebral level. Optimal thresholds for body composition changes were determined using the Shapley Additive Explanations (SHAP) method and validated using a Cox proportional hazard model.

Key findings and limitations: Changes in SMI, SATI, and VATI were the three most important features for predicting all-cause mortality. SMI change was inversely associated with the all-cause mortality risk, and changes in the SATI and VATI showed a U-shaped relationship with the all-cause mortality risk. SMI loss ($\geq$4.0%), SATI gain ($\geq$15.0%), and VATI gain ($\geq$12.0%) were independently associated with an increased all-cause mortality risk (SMI loss: hazard ratio, 6.79, $p < 0.001$; SATI gain: hazard ratio: 2.95, $p = 0.002$; VATI gain: hazard ratio: 2.91, $p < 0.001$).

Conclusions and clinical implications: The thresholds determined in this study can help identify patients with considerable body composition changes after 6 mo of ADT and guide interventions to improve body composition.

† Equally contributing first authors.
* Corresponding author. Department of Radiation Oncology, MacKay Memorial Hospital, 92, Section 2, Chung Shan North Road, Taipei 104217, Taiwan. Tel. +886 2 2809 4661 #2301; Fax: +886 2 2809 618.
E-mail address: sinus.5706@mmh.org.tw (J. Lee).

https://doi.org/10.1016/j.euros.2024.10.007

Patient summary: We identified muscle loss and increased adipose tissue thresholds associated with all-cause mortality during androgen deprivation therapy for men with prostate cancer. These thresholds can help guide interventions to improve body composition and potentially improve outcomes.

1. Introduction

Prostate cancer is one of the most prevalent cancers in men, with approximately 1 466 680 new cases reported worldwide in 2022 [1]. Androgen deprivation therapy (ADT) with radiotherapy is crucial in improving the survival of men with prostate cancer. However, ADT can contribute to changes in body composition, such as reduced skeletal muscle mass and increased fat mass [2–5]. Body composition is a biomarker of overall health that provides prognostic information of men with prostate cancer [4–7]. Skeletal muscle and adipose tissues are endocrine organs that can produce myokines/adipokines to influence metabolism, immune surveillance, inflammation, and physical functions [8]. A meta-analysis revealed that men with lower muscle mass had a 50% greater all-cause mortality risk than those with higher muscle mass [6]. However, the thresholds for body composition changes associated with survival remain unclear. Clarifying such thresholds may assist in identifying patients with considerable body composition changes during ADT and therefore guide enhanced interventions that improve body composition.

The association between body composition changes and patient survival is potentially nonlinear and involves complex interactions. Therefore, determination of thresholds is challenging. With advancements in technology such as machine learning (ML) and explainable artificial intelligence (XAI), the optimal thresholds of body composition changes could be determined. ML algorithms can manage nonlinear relationships and complex interactions to predict outcomes [9–12]. The SHapley Additive Explanations (SHAP) method is used widely to interpret ML models by visualizing the importance of features and inexplicable workings of the models. Although XAI may help identify the thresholds of body composition changes [12–14], these techniques have not been applied to explore the association between body composition changes and survival of patients with prostate cancer.

Body composition changes can be assessed objectively using computed tomography (CT) at the third lumbar vertebra (L3) level during cancer treatment [4]. This study aimed to analyze body composition changes observed using CT at baseline and 6 mo after ADT initiation, and use ML models and XAI to determine the thresholds of body composition changes associated with all-cause mortality of men with prostate cancer (Fig. 1).

2. Patients and methods

2.1. Study population

We retrospectively reviewed the data of patients with newly diagnosed National Comprehensive Cancer Network (NCCN) intermediate- or high-risk prostate cancer who underwent radiotherapy (75–80 Gy) and concurrent luteinizing hormone-releasing hormone (LHRH) agonist treatment at MacKay Memorial Hospital (derivation cohort) or Changhua Christian Hospital (external validation cohort) between 2010 and 2019. The ADT durations were 6 mo and 2 yr for patients with intermediate- and high-risk prostate cancer, respectively. The inclusion criteria were available CT images (including those at the L3 vertebral level) obtained at baseline and 6 mo after ADT initiation. We excluded patients with any of the following conditions: (1) a history of prior malignancy and treatment, (2) insufficient clinical information, (3) a lack of follow-up data, (4) no CT scans at 6 mo after ADT initiation, or (5) inadequate quality of CT scans. Of the 650 patients who were screened (derivation cohort, 403 patients; external validation cohort, 247 patients), 538 patients (derivation cohort, 332 patients; external validation cohort, 206 patients) were enrolled in the analysis (Supplementary Fig. 1). Clinical data, including age, age-adjusted Charlson Comorbidity Index (CCI), tumor stage, Gleason score, and pretreatment prostate-specific antigen (PSA) level, were derived from the institutional database. This study was approved by our institutional review board, and the requirement for informed consent was waived because of the retrospective nature of this study. This study followed the reporting guidelines in TRIPOD (Transparent Reporting of a multivariate prediction model for Individual Prognosis Or Diagnosis) [15].

The primary outcome measure was all-cause mortality, which was defined as the time from the date of diagnosis to the date of death due to any cause or the last follow-up. The date and cause of death and the date of the last follow-up were derived from the institutional database. The secondary outcome measures were noncancer and cancer mortality. Noncancer mortality was defined as the time from the date of diagnosis to the date of death from causes other than prostate cancer or the last follow-up. Cancer mortality was defined as the time from diagnosis to the date of death from prostate cancer or the last follow-up.

2.2. Skeletal muscle measurement

CT images obtained at baseline and 6 mo after ADT initiation were retrieved for an analysis. The parameters of CT images included the following: contrast enhancement, 3-mm slice thickness, 120 kVp, and approximately 290 mA. A single axial CT image at L3 was used by a researcher who was blinded to the information of the patients to analyze the cross-sectional areas (cm^2) of the skeletal muscle and visceral and subcutaneous adipose tissues using 3D Slicer software (version 4.11). Body composition was

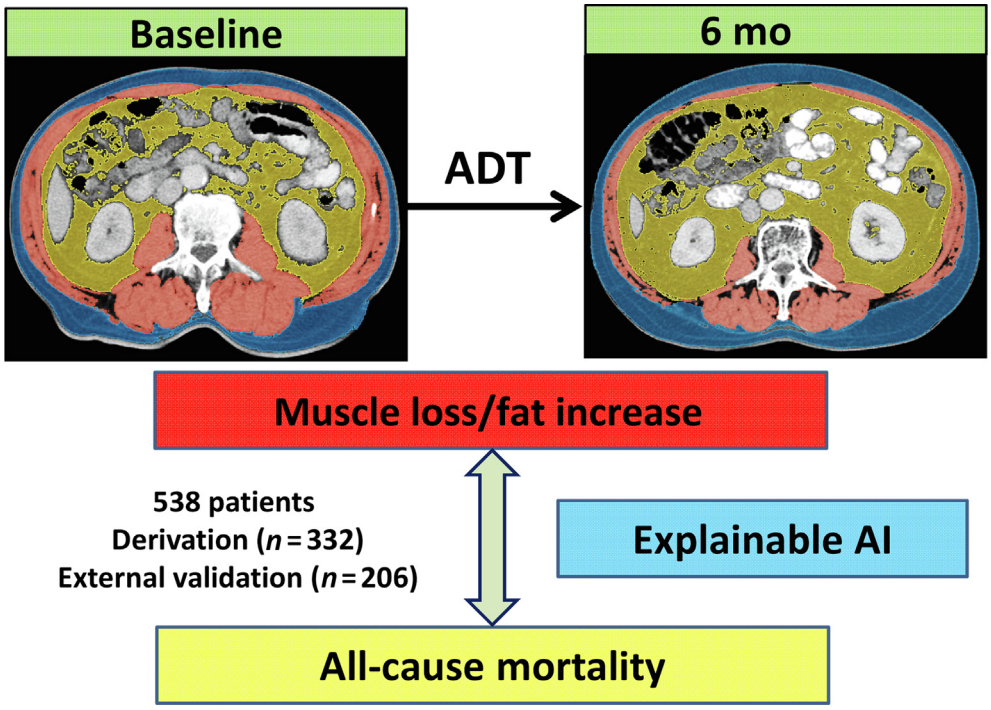

Fig. 1 – Utilization of explainable AI to explore the threshold of body composition change for all-cause mortality during androgen deprivation therapy. Body composition was assessed on a transversal computed tomography slice at the level of L3. ADT = androgen deprivation therapy; AI = artificial intelligence.

delineated based on Hounsfield unit (HU) thresholds, which ranged from −29 to +150 HU for skeletal muscle (including the psoas, rectus abdominis, paraspinal, transversus abdominis, and internal and external oblique muscles), −50 to −150 HU for visceral adipose tissue, and −30 to −190 HU for subcutaneous tissue [16]. The cross-sectional areas of the body composition were normalized to the patient's height to calculate the skeletal muscle index (SMI), subcutaneous adipose tissue index (SATI), and visceral adipose tissue index (VATI) (cm^2/m^2). Relative changes in body composition parameters were calculated as follows:

$$Bodycomposition\,change(\%) = \frac{Bodycomposition_{SecondCT} - Bodycomposition_{FirstCT}}{Bodycomposition_{FirstCT}} \times 100$$

2.3. Machine learning models

The ML algorithms are summarized in Supplementary Figure 1. The derivation cohort was used to train the models and identify the thresholds of body composition changes associated with all-cause mortality, whereas the external validation cohort was used to validate the thresholds. The features potentially associated with all-cause mortality were selected based on the domain expertise, including age, CCI, tumor stage, Gleason score, PSA level, and body composition parameters [3–7,17]. The features were rescaled based on the z scores for data standardization.

Three ML algorithms, Random Forest (RF), eXtreme Gradient Boosting (XGBoost), and Categorical Boosting (CatBoost), were trained to predict all-cause mortality using the Python Scikit-learn library (version 1.4.0; https://github.com/scikit-learn/scikit-learn.git), XGBoost (version 2.0.3; https://github.com/dmlc/xgboost.git), and CatBoost (version 1.2.2; https://github.com/catboost/catboost.git) [18]. The borderline-synthetic minority oversampling technique (borderline-SMOTE) was applied to address the effects of imbalanced data. Hyperparameter tuning was performed using randomized search parameter settings with 200 iterations and evaluated using ten-fold cross-validation targeting to maximize the area under the curve (AUC). The AUC, F1 score, sensitivity, specificity, and accuracy were evaluated using 500 bootstraps of the derivation cohort and recorded with their 95% confidence intervals (CIs). The efficacy of the three ML algorithms was assessed using an external validation cohort. Ultimately, the optimal model was utilized for subsequent interpretation using the SHAP method.

2.4. SHAP visualizations

The SHAP value for each feature within the model was calculated to evaluate the association between input features and all-cause mortality. To visualize global features and effects in the model, SHAP importance and summary plots were generated. SHAP dependence plots were created to interpret the relationship between the features and the model's prediction. In the SHAP dependence plots, real feature values were plotted on the *x* axis and SHAP values were plotted on the *y* axis. SHAP values of >0 corresponded to a positive class prediction in the model, indicating a higher risk of all-cause mortality. Therefore, the threshold could be identified based on where the SHAP values exceeded zero [12–14]. The SHAP method was implemented using Python with SHAP version 0.40.0.

2.5. Statistical analysis

Continuous data are presented as means and standard deviations, or medians and interquartile ranges (IQRs). Categorical data are presented as counts and percentages. The independent *t* test or Mann-Whitney U test was performed to compare continuous variables, and the chi-square test was performed to compare categorical variables, as statistically appropriate. A paired *t* test was performed to evaluate changes in body composition.

Cox proportional hazard models were used to estimate hazard ratios (HRs) and 95% CIs. Multivariable models were selected using backward elimination with a 0.10 significance level of inclusion. Data were analyzed using IBM SPSS software (version 21.0; IBM Corp., Armonk, NY, USA). Statistical significance was set at $p < 0.05$.

3. Results

3.1. Patient characteristics

A total of 538 patients with a median age of 71 yr (IQR, 65–77 yr) were enrolled in the analysis. Table 1 presents patient characteristics. No statistically significant difference in age, CCI score, tumor stage, Gleason score, and PSA level were observed between cohorts. In the derivation cohort, the median follow-up period was 69.5 mo (IQR, 48.6–109.9 mo), with 72 (21.7%) deaths recorded (noncancer death: 49; cancer death: 23), while the median follow-up period in the external validation cohort was 71.3 yr (IQR, 50.3–109.0 yr), with 46 (22.3%) deaths recorded (noncancer death: 32; cancer death: 14).

Table 1 – Patient and tumor characteristics[a]

Characteristics	Derivation cohort (n = 332)	External validation cohort (n = 206)	p value
Age (yr), median (IQR)	71 (66–77)	72 (65–76)	0.82
Age-adjusted CCI			0.77
1–2	68 (20.5)	44 (21.4)	
3–4	154 (46.4)	89 (43.2)	
5–7	110 (33.1)	73 (35.4)	
T stage			0.99
T1	82 (24.7)	49 (23.8)	
T2	151 (45.5)	94 (45.6)	
T3	76 (22.9)	48 (23.3)	
T4	23 (6.9)	15 (7.3)	
Gleason score			0.97
6	64 (19.3)	39 (18.9)	
7	122 (36.7)	80 (38.8)	
8	74 (22.3)	45 (21.8)	
9	61 (18.4)	37 (18.0)	
10	11 (3.3)	5 (2.4)	
PSA level (ng/ml), median (IQR)	23.7 (14.7–43.0)	23.3 (15.7–41.3)	0.47
NCCN risk group			0.58
Intermediate	80 (24.1)	54 (26.2)	
High	252 (75.9)	152 (73.8)	
BMI (kg/m^2)			
Before treatment	24.3 ± 3.3	24.2 ± 3.3	0.78
After treatment	24.9 ± 3.5	24.8 ± 3.5	0.82
Change (%)	2.3 ± 3.4	2.3 ± 3.0	0.90
SMI (cm^2/m^2)			
Before treatment	45.9 ± 7.8	45.7 ± 7.6	0.73
After treatment	44.0 ± 7.7	44.1 ± 7.7	0.90
Change (%)	−4.1 ± 5.3	−3.5 ± 4.0	0.16
SATI (cm^2/m^2)			
Before treatment	41.5 ± 14.7	40.9 ± 13.6	0.67
After treatment	44.4 ± 15.6	43.5 ± 14.4	0.49
Change (%)	7.6 ± 9.4	6.5 ± 8.5	0.16
VATI (cm^2/m^2)			
Before treatment	53.0 ± 27.3	52.5 ± 25.8	0.83
After treatment	55.8 ± 28.4	55.1 ± 26.9	0.78
Change (%)	6.2 ± 11.0	5.5 ± 9.3	0.44

BMI = body mass index; CCI = Charlson Comorbidity Index; IQR = interquartile range; NCCN = National Comprehensive Cancer Network; PSA = prostate-specific antigen; SATI = subcutaneous adipose tissue index; SMI = skeletal muscle index; VATI = visceral adipose tissue index.
[a] Data are presented as mean ± standard deviation or *n* (%).

3.2. Body composition changes

The median durations between CT images were 182 d (IQR, 177–186 d) and 183 d (IQR, 176–186 d) for the derivation and external validation cohorts, respectively ($p = 0.70$). The SMI decreased by 4.1% in the derivation cohort ($p < 0.001$) and 3.5% in the external validation cohort ($p < 0.001$). The SATI and VATI increased by 7.6% and 6.2% in the derivation cohort ($p < 0.001$), and 6.5% and 5.5% in the external validation cohort ($p < 0.001$), respectively. No statistically significant differences in the parameters of the body composition changes were observed between cohorts (Table 1).

3.3. Model performance and interpretation

In the derivation cohort, the RF, XGBoost, and CatBoost models had favorable performances, with AUCs of 0.881 (95% CI, 0.879–0.884), 0.864 (95% CI, 0.862–0.866), and 0.890 (95% CI, 0.888–0.892), respectively (Supplementary Fig. 2 and Supplementary Table 1). In the external validation cohort, the CatBoost model had the highest AUC of 0.970, and the RF and XGBoost models had AUCs of 0.955 and 0.880, respectively. Therefore, the CatBoost model was selected for the downstream SHAP analysis.

The SHAP summary and importance plots present a global explanation of the model at the feature level and rank the importance of the features to the prediction. Results from XAI indicated that the three most important features for predicting all-cause mortality were changes in SMI, SATI, and VATI; baseline muscle and adipose tissues were of lesser importance (Supplementary Fig. 3). The SHAP dependence plots showed the relationships between body composition changes and all-cause mortality (Fig. 2). In both cohorts, the SMI change was inversely correlated with the SHAP values, indicating that a decreased SMI following ADT was associated with a higher risk of all-cause mortality. Notably, in both cohorts, the SMI change exceeded the SHAP value of 0 by approximately −4.0%. This may serve as the optimal threshold for muscle loss associated with an increased all-cause mortality risk. In both cohorts, changes in the SATI and VATI showed a U-shaped relationship with the all-cause mortality risk. SATI gain of ≥15.0% or loss of ≥5.0% was associated with an increased all-cause mortality risk. VATI gain of ≥12.0% or loss of ≥5.0% was associated with an increased all-cause mortality risk.

Baseline SMI was inversely correlated with the risk of all-cause mortality (Supplementary Fig. 4) and exceeded SHAP

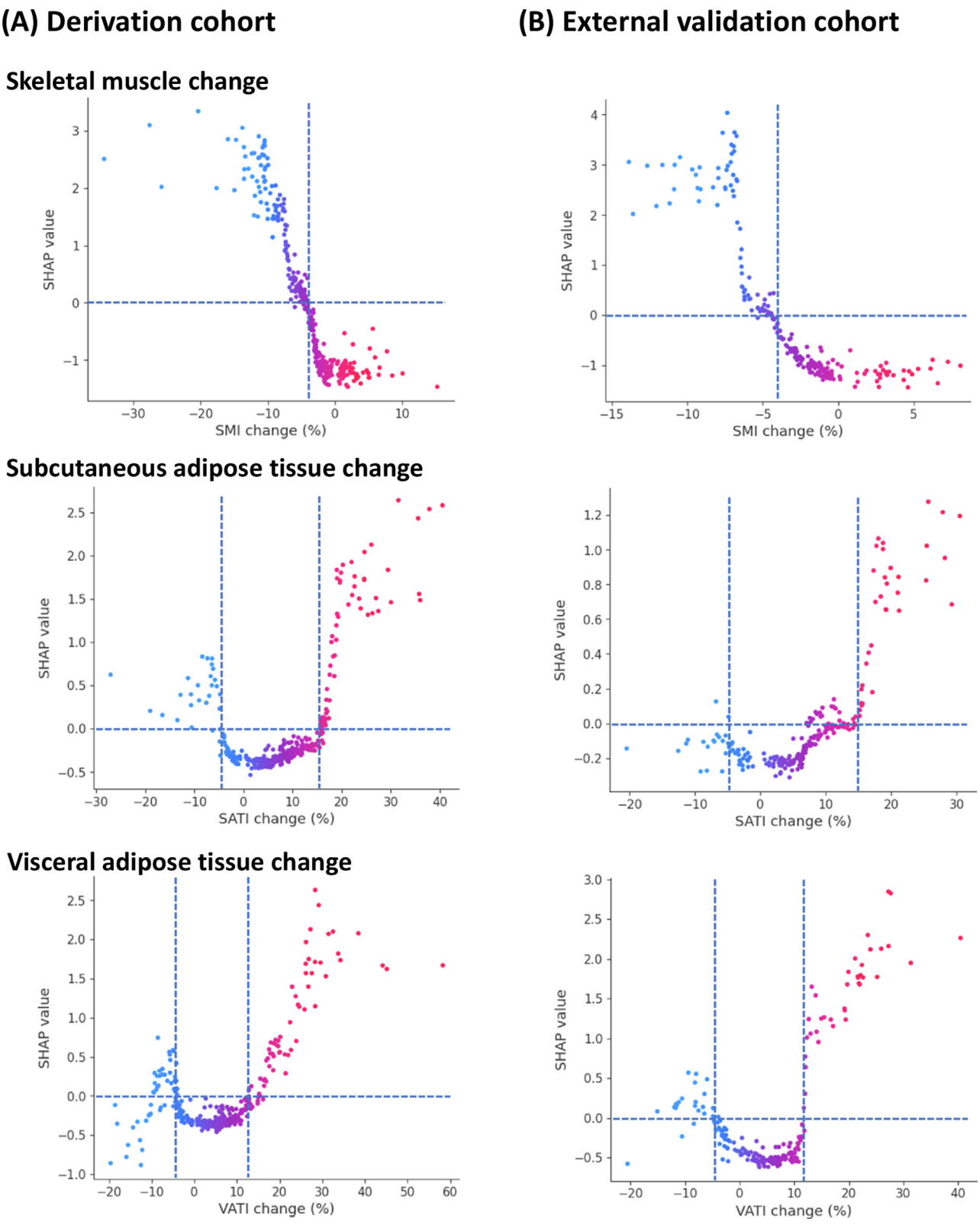

Fig. 2 – SHAP dependence plots of the CatBoost model in the (A) derivation and (B) external validation cohorts. Each dot represents a SHAP value for a feature per patient, and red to blue colors represent the feature's value from high to low, respectively. SHAP values for specific features exceeding zero represent an increased risk of all-cause mortality. SATI = subcutaneous adipose tissue index; SHAP = Shapley Additive Explanations; SMI = skeletal muscle index; VATI = visceral adipose tissue index.

value 0 by approximately 45.0 cm^2/m^2, which was identified as the cutoff value for pretreatment sarcopenia. The distribution of baseline SATI and VATI widely crossed the line of SHAP value of 0; therefore, the thresholds of these values could not be identified.

3.4. Validation of thresholds using Cox regression

Based on these thresholds, 268 (49.8%) patients in the overall cohort had pretreatment sarcopenia and 237 (44.1%) had SMI loss of ≥4.0% after 6 mo of ADT. Additionally, 102 (19.0%) and 40 (7.4%) patients comprised the SATI gain of ≥15.0% and SATI loss of ≥5.0% groups, respectively, and 110 (20.4%) and 60 (11.2%) patients comprised the VATI gain of ≥12.0% and VATI loss of ≥5.0% groups, respectively. According to the pretreatment sarcopenia status, the body composition changes were not significantly different between groups (Supplementary Table 2).

Patients in the pretreatment sarcopenia group had lower 5-yr overall survival, non–cancer-specific survival, and cancer-specific survival than patients in the nonsarcopenia group (overall survival: 80.2% vs 89.6%; $p < 0.001$; non–cancer-specific survival: 85.5% vs 92.0%; $p = 0.006$; cancer-specific survival: 93.3% vs 97.5%; $p = 0.003$; Supplementary Fig. 5). The SMI loss of ≥4.0% group had lower 5-yr overall survival than that of the SMI-maintained group (70.0% vs 97.4%; $p < 0.001$; Fig. 3). The group with SATI/VATI maintained had higher 5-yr overall survival than the group with SATI/VATI gain or loss.

Non–cancer-specific and cancer-specific survival based on the body composition changes are shown in Supplementary Figure 6. SMI loss of ≥4.0% was associated with lower non–cancer-specific and cancer-specific survival. SATI/VATI gain was associated with lower non–cancer-specific and cancer-specific survival, whereas SATI/VATI loss was associated with lower cancer-specific survival.

In the univariable analysis, age, CCI, tumor stage, Gleason score, PSA, body mass index change, pretreatment sarcopenia, and changes in the SMI, SATI, and VATI were associated with all-cause mortality (Table 2). Baseline SATI and VATI were not associated with all-cause mortality. In the multivariable analysis, SMI loss ≥4.0%, SATI gain ≥15.0%, and VATI gain ≥12.0% were independently associated with an increased all-cause mortality risk (SMI loss: HR, 6.79; 95% CI, 3.81–12.10; $p < 0.001$; SATI gain: HR, 2.95; 95% CI, 1.47–5.92; $p = 0.002$; VATI gain: HR, 2.91; 95% CI, 1.80–4.71; $p < 0.001$). Pretreatment sarcopenia and SATI/VATI loss ≥5.0% were not independently associated with all-cause mortality.

The subgroup analysis based on NCCN prostate cancer risk indicated that the high-risk group ($n = 404$) was more likely to experience SMI loss, SATI gain/loss, and VATI gain/loss than the intermediate-risk group ($n = 134$; Supplementary Table 3). Compared with patients in the intermediate-risk group, those in the high-risk group were older and had a higher CCI. For both the intermediate-risk and the high-risk group, SMI loss, SATI gain of ≥15.0%, and VATI gain of ≥12.0% were associated with lower overall survival (Supplementary Fig. 7). SATI/VATI loss was not associated with lower overall survival for patients in the intermediate-risk group; however, SATI/VATI loss was associated with lower overall survival for patients in the high-risk group.

The multivariable analysis of noncancer mortality revealed that SMI loss of ≥4.0%, SATI gain of ≥15.0%, and VATI gain of ≥12.0% were independently associated with an increased noncancer mortality risk (Supplementary Table 4), whereas pretreatment sarcopenia and SATI/VATI loss were not associated with the noncancer mortality risk. The multivariable analysis of cancer mortality revealed that SMI loss of ≥4.0%, SATI loss of ≥5.0%, and VATI loss of ≥5.0% were independently associated with an increased cancer mortality risk (Supplementary Table 5), whereas pretreatment sarcopenia and SATI/VATI gain were not associated with the cancer mortality risk.

4. Discussion

To the best of our knowledge, this study is the first to use XAI to determine the thresholds of body composition changes associated with all-cause mortality of men with prostate cancer. In this study, patients received 6 mo of ADT and experienced muscle loss and increased adipose tissue. Changes in SMI, SATI, and VATI were the three most important features for predicting all-cause mortality. The thresholds of body composition changes associated with all-cause mortality were validated externally and analyzed among subgroups based on risk groups. SMI loss of ≥4.0%, SATI gain of ≥15.0%, and VATI gain of ≥12.0% were independently associated with an increased all-cause mortality risk.

Reduced muscle mass and increased fat mass are associated with survival in patients with prostate cancer [3–7]. However, previous studies used Cox proportional hazard regression, a statistical method that had limited capacity to rank feature importance or determine the threshold of body composition changes associated with survival. Here, we applied XAI to identify cutoffs for pretreatment sarcopenia and body composition changes. Previous studies have reported that pretreatment sarcopenia was associated with an increased all-cause mortality risk [6,7], but did not evaluate the prognostic role of body composition changes. In this study, pretreatment sarcopenia was not independently associated with an increased all-cause mortality risk; however, SMI loss and SATI/VATI gain were independently associated with all-cause mortality. Furthermore, pretreatment sarcopenia was also not associated with body composition changes during ADT. These findings highlight the clinical relevance of preventing muscle loss and fat accumulation during ADT.

Commencing exercise after the initiation of ADT may preserve muscle mass and decrease fat mass [19]. The thresholds determined in this study may help guide enhanced multimodal interventions, including exercise, nutrition, and other anti-inflammatory interventions, during ADT to improve body composition. Combining exercise (both aerobic and resistance) with prolonged exercise durations could increase muscle mass and decrease body fat mass [19–21]. Supervised exercise could also improve cardiorespiratory fitness, maximal leg strength, and functional capacity [22]. Combining exercise and nutrition

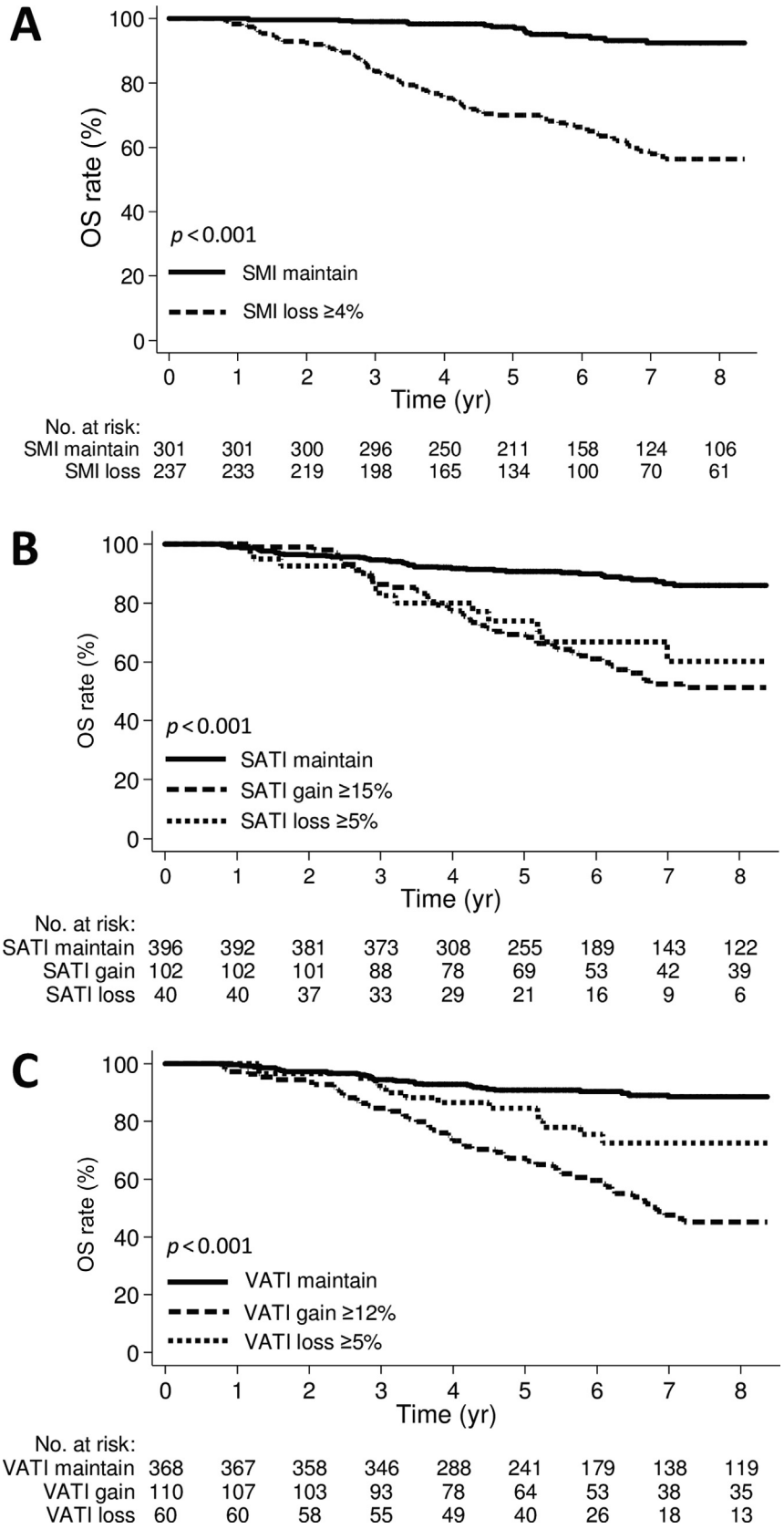

Fig. 3 – Kaplan-Meier curves demonstrating overall survival according to the thresholds of (A) SMI change, (B) SATI change, and (C) VATI change in the overall cohort. OS = overall survival; SATI = subcutaneous adipose tissue index; SMI = skeletal muscle index; VATI = visceral adipose tissue index.

Table 2 – Cox proportional hazard model for all-cause mortality in the overall cohort (n = 538)

Variable	Univariable		Multivariable [a]	
	Hazard ratio (95% CI)	p value	Hazard ratio (95% CI)	p value
Age (yr)	1.07 (1.04–1.10)	<0.001	–	–
Age-adjusted CCI (reference: 1–2)				
3–4	0.91 (0.50–1.66)	0.76	1.93 (0.97–3.82)	0.06
5–7	3.46 (2.01–5.96)	<0.001	3.87 (2.11–7.10)	<0.001
T stage (reference: T1)				
T2	1.48 (0.88–2.48)	0.14	1.06 (0.62–1.83)	0.82
T3	1.34 (0.75–2.39)	0.32	0.79 (0.43–1.45)	0.45
T4	4.99 (2.68–9.29)	<0.001	4.69 (2.29–9.61)	<0.001
Gleason score, continuous	1.90 (1.61–2.25)	<0.001	1.47 (1.23–1.77)	<0.001
PSA level, continuous	1.006 (1.003–1.009)	<0.001	1.006 (1.002–1.011)	0.006
BMI at baseline (1 kg/m^2 increase)	0.96 (0.91–1.02)	0.18	–	–
BMI change (per 1% increase)	1.11 (1.04–1.19)	0.001	–	–
Pretreatment sarcopenia [b]	2.02 (1.39–2.94)	<0.001	1.21 (0.81–1.80)	0.35
SMI loss ≥4.0% (vs SMI maintain)	9.01 (5.44–14.91)	<0.001	6.79 (3.81–12.10)	<0.001
SATI at baseline (1 cm^2/m^2 increase)	1.00 (0.98–1.01)	0.56	–	–
SATI change (reference: SATI maintain)				
SATI gain ≥15.0%	4.58 (3.12–6.72)	<0.001	2.95 (1.47–5.92)	0.002
SATI loss ≥5.0%	3.05 (1.65–5.63)	<0.001	1.29 (0.80–2.09)	0.29
VATI at baseline (1 cm^2/m^2 increase)	1.00 (0.99–1.01)	0.73	–	–
VATI change (reference: VATI maintain)				
VATI gain ≥12.0%	6.10 (4.10–9.10)	<0.001	2.91 (1.80–4.71)	<0.001
VATI loss ≥5.0%	2.53 (1.39–4.58)	0.002	1.65 (0.86–3.16)	0.13

BMI = body mass index; CI = confidence interval; CCI = Charlson Comorbidity Index; PSA = prostate-specific antigen; SATI = subcutaneous adipose tissue index; SMI = skeletal muscle index; VATI = visceral adipose tissue index.
[a] Multivariable analysis using a backward selection method.
[b] SMI <45.0 cm^2/m^2 was defined as sarcopenia.

interventions appeared to decrease waist circumference effectively; however, interventions comprising only exercise may increase lean mass and decrease body fat mass more effectively [23]. Additionally, skeletal muscle and adipose tissue inflammation may create a vicious cycle by producing myokines and adipokines that trigger muscle loss and increases in adipose tissue [24]. Anti-inflammatory interventions including exercise or medications may mitigate the detrimental effects of the deleterious cycle comprising adipose tissue and muscle inflammation and help increase muscle and decrease adipose tissue [25]. However, we were unable to determine a causal relationship between body composition changes and mortality; we were only able to reveal an association between these. Further studies are necessary to evaluate whether enhanced interventions that improve body composition during ADT can improve outcomes.

The U-shape relationship between changes in the SATI and VATI and the all-cause mortality risk may be explained by further analyses based on cancer and noncancer mortality. Multivariable analyses revealed that SATI/VATI loss was independently associated with an increased cancer mortality risk, whereas SATI/VATI increase was independently associated with an increased noncancer mortality risk. These findings suggest that adipose tissue loss is a sign of cancer cachexia and a predictor of cancer mortality [26]. Adipose tissue, which is an endocrine organ, secretes adipokines that regulate the metabolism and immune system [8]. Therefore, we suggest that maintaining adipose tissue during ADT may preserve its functions and optimize survival outcomes.

This study included patients with intermediate-risk and high-risk prostate cancer. Patients in the high-risk group were more likely to experience SMI loss, SATI gain/loss, and VATI gain/loss after 6 mo of ADT than those in the intermediate-risk group. This may be explained by multiple factors such as advanced disease, older age, and more comorbidities, which may be associated with muscle loss and adipose tissue gain/loss during treatment [27]. We also observed inconsistent effects of SATI/VATI loss on overall survival among intermediate-risk and high-risk groups. Notably, the intermediate-risk group comprised few patients with SATI/VATI loss (n = 4/n = 7), and these patients did not experience mortality events. Hence, a lack of statistical power likely limited our ability to test the prognostic impact of SATI/VATI loss on intermediate-risk patients. Further studies with a larger intermediate-risk group are required to validate the prognostic significance of body composition changes during ADT for these patients.

In addition to abdominal CT imaging, dual-energy x-ray absorptiometry (DXA) is another recommended technique for objective measures of body composition [20]. Skeletal muscle and adipose tissue areas measured using CT at L3 were highly correlated with the total body skeletal muscle and adipose tissue measured using DXA (skeletal muscle: r = 0.94; adipose tissue: r = 0.88) [16]. However, the reliability of DXA may vary according to the trunk thickness and may have lower accuracy when used to assess longitudinal changes in body composition [28]. Therefore, we suggest that further studies are required to validate whether the identified thresholds actually apply to DXA-measured body composition.

This study has some limitations. This study was retrospective in nature and may have residual confounding factors that were not fully accounted for. Several potentially important features, including serum testosterone levels, physical activity, muscle strength, and nutritional status, of most patients were not available. This study analyzed

body composition changes after 6 mo of ADT only; therefore, the prognostic value of subsequent body composition changes could not be evaluated. A longitudinal study with more time points may provide more comprehensive information. Moreover, the effects of androgen receptor signaling inhibitor (ARSI)-induced body composition changes on survival could not be evaluated because the patients in this study were treated with radiotherapy and LHRH agonists. This topic should be investigated in further studies because the effects of ARSIs on body composition changes may be distinct from those of LHRH agonists [29].

5. Conclusions

In conclusion, our study provides evidence that XAI can facilitate the investigation of the relationship between body composition changes and survival, and identify the optimal thresholds of body composition changes. Changes in muscle and adipose tissue after 6 mo of ADT are important features for predicting all-cause mortality in patients with prostate cancer. SMI loss of $\geq$4.0%, SATI gain of $\geq$15.0%, and VATI gain of $\geq$12.0% were independently associated with an increased all-cause mortality risk and may be the optimal thresholds for predicting all-cause mortality. Our results may help clinicians identify patients with considerable body composition changes after 6 mo of ADT and may guide interventions for these patients, thereby potentially improving survival outcomes.

Author contributions: Jie Lee had full access to all the data in the study and takes responsibility for the integrity of the data and the accuracy of the data analysis.

Study concept and design: Lee.
Acquisition of data: Chiang, J.-B. Lin, Tsai.
Analysis and interpretation of data: Chen, Chiang, J.-B. Lin, Tsai, W.-C. Lin, Jan, Wu, Lee.
Drafting of the manuscript: Chen, Chiang.
Critical revision of the manuscript for important intellectual content: Chen, Chiang, J.-B. Lin, Tsai, W.-C. Lin, Jan, Wu, Lee.
Statistical analysis: J.-B. Lin, Lee.
Obtaining funding: Wu, Lee.
Administrative, technical, or material support: Chen, Wu, Lee.
Supervision: Lee.
Other: None.

Financial disclosures: Jie Lee certifies that all conflicts of interest, including specific financial interests and relationships and affiliations relevant to the subject matter or materials discussed in the manuscript (eg, employment/affiliation, grants or funding, consultancies, honoraria, stock ownership or options, expert testimony, royalties, or patents filed, received, or pending), are the following: None.

Funding/Support and role of the sponsor: This work was supported by the National Science and Technology Council Taiwan (grant numbers: contract no. MOST 110-2314-B-195-033, MOST 110-2314-B-A49A-506-MY3, NSTC 113-2314-B-195-011-MY3) and MacKay Memorial Hospital (grant numbers: MMH-113-53, MMH-113-109).

Ethics statement: This study was conducted in accordance with the Declaration of Helsinki. This study was approved by Institutional Review Board of MacKay Memorial Hospital (20MMHIS213e) and Changhua Christian Hospital (230329).

Data sharing: The datasets used and/or analyzed during the current study are available from the corresponding author on reasonable request.

Appendix A. Supplementary data

Supplementary data to this article can be found online at https://doi.org/10.1016/j.euros.2024.10.007.

References

[1] Bray F, Laversanne M, Sung H, et al. Global cancer statistics 2022: GLOBOCAN estimates of incidence and mortality worldwide for 36 cancers in 185 countries. CA Cancer J Clin 2024;74:229–63.
[2] Smith MR, Finkelstein JS, McGovern FJ, et al. Changes in body composition during androgen deprivation therapy for prostate cancer. J Clin Endocrinol Metab 2002;87:599–603.
[3] Nguyen PL, Alibhai SM, Basaria S, et al. Adverse effects of androgen deprivation therapy and strategies to mitigate them. Eur Urol 2015;67:825–36.
[4] Chiang PK, Tsai WK, Chiu AW, Lin JB, Yang FY, Lee J. Muscle loss during androgen deprivation therapy is associated with higher risk of non-cancer mortality in high-risk prostate cancer. Front Oncol 2021;11:722652.
[5] Leong DP, Fradet V, Niazi T, et al. Adiposity and Muscle Strength in Men With Prostate Cancer and Cardiovascular Outcomes. JACC: CardioOncology 2024;6(5):761–71.
[6] Lopez P, Newton RU, Taaffe DR, et al. Associations of fat and muscle mass with overall survival in men with prostate cancer: a systematic review with meta-analysis. Prostate Cancer Prostatic Dis 2022;25:615–26.
[7] McDonald AM, DeMora L, Yang ES, et al. Body composition and mortality in men receiving prostate radiotherapy: a pooled analysis of NRG/RTOG 9406 and NRG/RTOG 0126. Cancer 2023;129:685–96.
[8] Severinsen MCK, Pedersen BK. Muscle-organ crosstalk: the emerging roles of myokines. Endocr Rev 2020;41:594–609.
[9] Yoon HG, Oh D, Noh JM, et al. Machine learning model for predicting excessive muscle loss during neoadjuvant chemoradiotherapy in oesophageal cancer. J Cachexia Sarcopenia Muscle 2021;12:1144–52.
[10] Hsu WH, Ko AT, Weng CS, et al. Explainable machine learning model for predicting skeletal muscle loss during surgery and adjuvant chemotherapy in ovarian cancer. J Cachexia Sarcopenia Muscle 2023;14:2044–53.
[11] Lin WC, Weng CS, Ko AT, et al. Interpretable machine learning model based on clinical factors for predicting muscle radiodensity loss after treatment in ovarian cancer. Support Care Cancer 2024;32:544.
[12] Li R, Shinde A, Liu A, et al. Machine learning-based interpretation and visualization of nonlinear interactions in prostate cancer survival. JCO Clin Cancer Inform 2020;4:637–46.
[13] Ladbury C, Li R, Shiao J, et al. Characterizing impact of positive lymph node number in endometrial cancer using machine-learning: a better prognostic indicator than FIGO staging? Gynecol Oncol 2022;164:39–45.
[14] Ladbury C, Li R, Danesharasteh A, et al. Explainable artificial intelligence to identify dosimetric predictors of toxicity in patients with locally advanced non-small cell lung cancer: a secondary analysis of RTOG 0617. Int J Radiat Oncol Biol Phys 2023;117:1287–96.
[15] Collins GS, Reitsma JB, Altman DG, Moons KGM. Transparent reporting of a multivariable prediction model for individual prognosis or diagnosis (TRIPOD): the TRIPOD statement. Eur Urol 2015;67:1142–51.
[16] Mourtzakis M, Prado CM, Lieffers JR, Reiman T, McCargar LJ, Baracos VE. A practical and precise approach to quantification of body composition in cancer patients using computed tomography images acquired during routine care. Appl Physiol Nutr Metab 2008;33:997–1006.

[17] Stevens LM, Mortazavi BJ, Deo RC, Curtis L, Kao DP. Recommendations for reporting machine learning analyses in clinical research. Circ Cardiovasc Qual Outcomes 2020;13:e006556.
[18] Pedregosa F, Varoquaux G, Gramfort A, et al. Scikit-learn: machine learning in Python. J Mach Learn Res 2011;12:2825–30.
[19] Shao W, Zhang H, Qi H, Zhang Y. The effects of exercise on body composition of prostate cancer patients receiving androgen deprivation therapy: an update systematic review and meta-analysis. PLoS One 2022;17:e0263918.
[20] Newton RU, Galvão DA, Spry N, et al. Timing of exercise for muscle strength and physical function in men initiating ADT for prostate cancer. Prostate Cancer Prostatic Dis 2020;23:457–64.
[21] Pelzer F, Leisge K, Schlüter K, Schneider J, Wiskemann J, Rosenberger F. Effects of exercise mode and intensity on patient-reported outcomes in cancer survivors: a four-arm intervention trial. Support Care Cancer 2023;31:315.
[22] Harrison MR, Davis PG, Khouri MG, et al. A randomized controlled trial comparing changes in fitness with or without supervised exercise in patients initiated on enzalutamide and androgen deprivation therapy for non-metastatic castration-sensitive prostate cancer (EXTEND). Prostate Cancer Prostatic Dis 2022;25:58–64.
[23] Yang U, Harikrishna A, Preda V, Chen J. Efficacy of multidisciplinary interventions in preventing metabolic syndrome and improving body composition in prostate cancer patients treated with androgen deprivation therapy: a systematic review and meta-analysis. Clin Nutr ESPEN 2023;58:27–49.
[24] Kalinkovich A, Livshits G. Sarcopenic obesity or obese sarcopenia: a cross talk between age-associated adipose tissue and skeletal muscle inflammation as a main mechanism of the pathogenesis. Ageing Res Rev 2017;35:200–21.
[25] Slavin MB, Khemraj P, Hood DA. Exercise, mitochondrial dysfunction and inflammasomes in skeletal muscle. Biomed J 2024;47:100636.
[26] Luan Y, Zhang Y, Yu SY, et al. Development of ovarian tumour causes significant loss of muscle and adipose tissue: a novel mouse model for cancer cachexia study. J Cachexia Sarcopenia Muscle 2022;13:1289–301.
[27] Benzo RM, Moreno PI, Fox RS, et al. Comorbidity burden and health-related quality of life in men with advanced prostate cancer. Support Care Cancer 2023;31:496.
[28] Shah UA, Ballinger TJ, Bhandari R, et al. Imaging modalities for measuring body composition in patients with cancer: opportunities and challenges. J Natl Cancer Inst Monogr 2023;2023:56–67.
[29] Blow TA, Murthy A, Grover R, et al. Profiling of skeletal muscle and adipose tissue depots in men with advanced prostate cancer receiving different forms of androgen deprivation therapy. Eur Urol Open Sci 2023;57:1–7.